nature nanotechnology

REVIEW ARTICLE

PUBLISHED ONLINE: 31 JULY 2011 | DOI: 10.1038/NNANO.2011.102

Nanomechanics of functional and pathological amyloid materials

Tuomas P. J. Knowles[1]* and Markus J. Buehler[2,3,4]*

Amyloid or amyloid-like fibrils represent a general class of nanomaterials that can be formed from many different peptides and proteins. Although these structures have an important role in neurodegenerative disorders, amyloid materials have also been exploited for functional purposes by organisms ranging from bacteria to mammals. Here we review the functional and pathological roles of amyloid materials and discuss how they can be linked back to their nanoscale origins in the structure and nanomechanics of these materials. We focus on insights both from experiments and simulations, and discuss how comparisons between functional protein filaments and structures that are assembled abnormally can shed light on the fundamental material selection criteria that lead to evolutionary bias in multiscale material design in nature.

A wide range of natural and artificial peptides and proteins possess an intrinsic propensity to self-assemble into fibrillar nanostructures that are rich in β-sheet secondary structure. These fibrils are generally organized in a similar manner at the molecular level; they are characterized by β-strands that are oriented perpendicularly to the fibril axis, and connected through a dense hydrogen-bonding network, which results in supramolecular β-sheets that often extend continuously over thousands of molecular units[1–5] (Fig. 1). Such fibrillar structures first received attention through their association with diseases related to protein misfolding[6], including neurodegenerative disorders such as Alzheimer's and Parkinson's diseases[7,8], where normally soluble proteins are deposited pathologically into obdurate aggregates known as amyloid fibrils[9–14] (see Table 1 for an overview of key terminology and concepts). Subsequently, however, functional amyloid-like materials were discovered in varying roles throughout nature[15–20]. Moreover, under conditions where the natively folded states of proteins are thermodynamically destabilized, a wide range of unrelated peptides and proteins have been observed to form artificial fibrillar materials *in vitro* that are characterized by a quaternary amyloid structure and this has led to the design of functional nanomaterials.

Amyloid materials, which are present in cells and in the extracellular space, represent a class of nanoscale structures that have various functional and pathological roles (Table 2; Fig. 2)[15–17,19,21]. As such, amyloid nanostructures are increasingly viewed as a general alternative form of protein structure that is different from, but in many cases no less organized than, the native states of proteins[1,22]. Moreover, this type of structure does not depend primarily on highly evolved side-chain interactions, but rather on universal physical and chemical characteristics that are inherent in the nature of all polypeptide molecules such as the propensity for hydrogen bonding in the backbone[23].

Understanding why certain material characteristics have been conserved or refined over millions of years of evolution underlies many fundamental questions in biology, but this knowledge is also required to develop methods for using artificial proteinaceous nanostructures as practical functional materials. The question of material selection becomes particularly intriguing from a technological viewpoint because many protein materials are formed from scarce amounts of building blocks (that is, small volumes of material), from a few distinct building blocks (for example, only 20 natural amino acids) and from weak bonding (for example, hydrogen bonding), and are typically formed under severe energy constraints[24]. Because amyloid materials consist of generic assemblies of normally soluble proteins bound together in a simple periodic structure defined by main-chain hydrogen-bonding constraints, studying them should shed new light on the material selection criteria that shape more complex proteinaceous materials in nature.

Nanomechanics of amyloid materials

Mechanical properties are critical to our understanding of how materials contribute to a biological or synthetic system. These properties include the strength of adhesive forces between fibrils or their surrounding, their rigidity, or the maximum stress that they can sustain without breaking. In common with many biological materials, amyloid materials have hierarchical structures (Fig. 1a) from the molecular to the macroscopic scale. Mechanical testing on the nanoscale allows the study of amyloid materials on the single fibril level and provides the ability to directly probe the forces that bind individual proteins together in such materials.

Nanomechanical testing can be performed by using atomic force microscopy (AFM) to carry out indentation measurements with high lateral resolution. Measurements of the contact stiffness of phenylalanine nanofibrils using this method showed that they are characterized by a Young's modulus (E) of 19 GPa (ref. 25), implying a comparatively high stiffness (Fig. 3). This type of nanomechanical manipulation by AFM also allows the miniaturization of standard three-point bending testing. To this effect, the nanofibril structures are suspended over nanoscale gaps and an AFM tip is used to load the beam[26,27]. Experiments probing fibrils assembled from the protein insulin yield $E = 3.3 \pm 0.4$ GPa (ref. 28). For nanofibrils with smaller diameters of only a few nanometres, it can be more challenging to probe their mechanical properties by directly applying a force and measuring resulting displacements because they are more fragile and flexible. Therefore, alternative methods to probe mechanical properties have been applied.

[1]Department of Chemistry, University of Cambridge, Lensfield Road, Cambridge CB2 1EW, UK, [2]Laboratory for Atomistic and Molecular Mechanics, Department of Civil and Environmental Engineering, Massachusetts Institute of Technology, 77 Massachusetts Ave. Room 1-235A&B, Cambridge, Massachusetts, USA, [3]Center for Computational Engineering, Massachusetts Institute of Technology, 77 Massachusetts Ave., Cambridge, Massachusetts, USA, [4]Center for Materials Science and Engineering, Massachusetts Institute of Technology, 77 Massachusetts Ave., Cambridge, Massachusetts, USA. *e-mail: tpjk2@cam.ac.uk; mbuehler@MIT.EDU

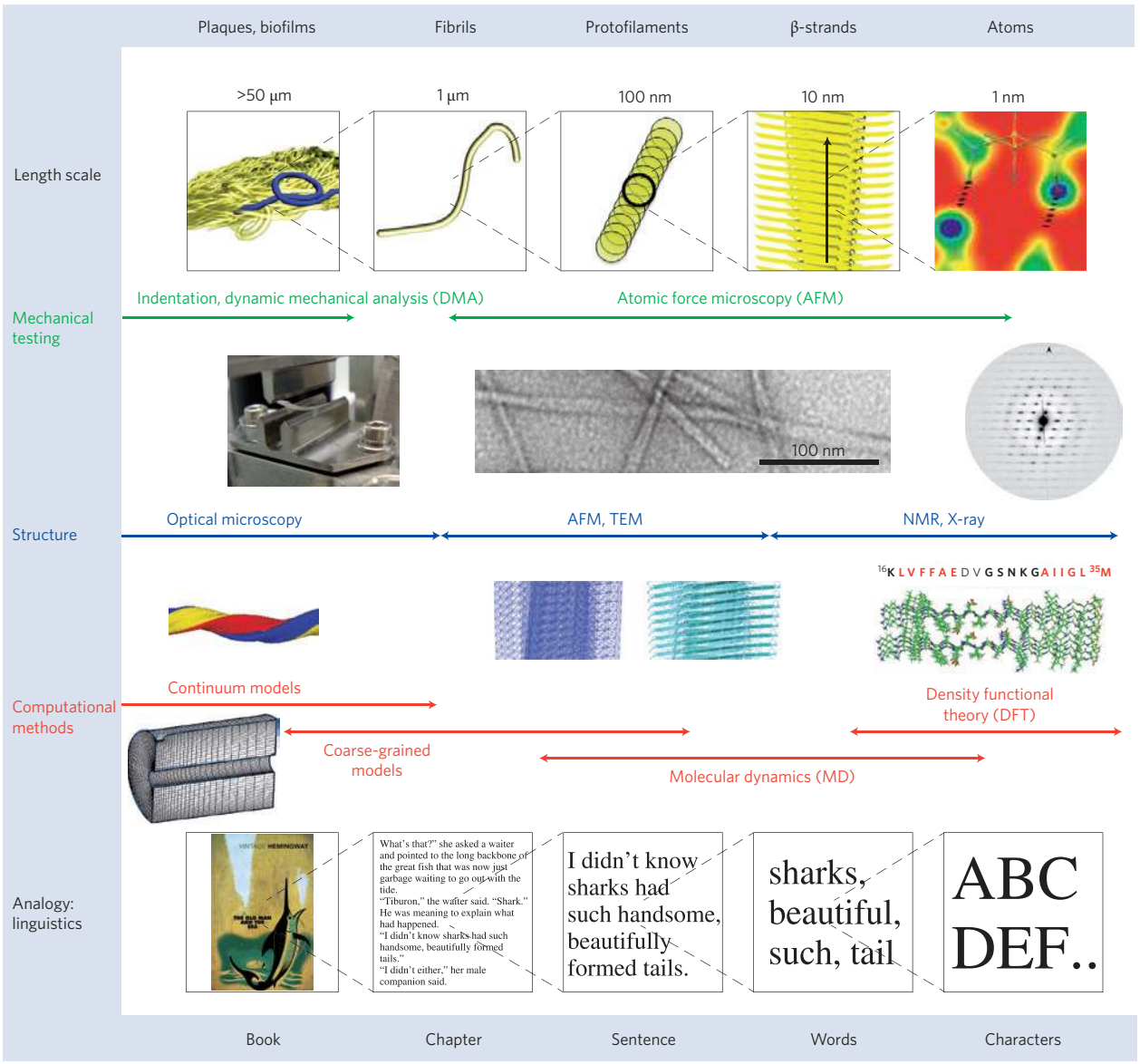

Figure 1 | The hierarchical structure of amyloid materials. Upper panel: Five different levels of hierarchy in the structure of amyloid materials. Second and third panels: Different experimental and computational analysis tools for studying the mechanical properties and structure of amyloid materials on the different length scales. Second panel: The image on the left shows an artificial amyloid film being tested in a DNA setup. The transmission electron micrograph represents an Alzheimer's amyloid β-fibril. The image on the right shows the diffraction pattern from amyloid-like nanocrystals formed from the peptide GNNQQNY from the N-terminal region of the yeast prion protein Sup35. Figures in the second panel reproduced with permission from: left, ref. 93, © 2010 NPG; middle, ref. 14, © 2008 NAS; right, ref. 102, © 2003 Elsevier. Third panel: The inlay above 'Continuum models' represents a large-scale atomistic model of an Alzheimer's β-amyloid fibril; the image above 'Coarse-grained models' shows a coarse-grained elastic network model of an amyloid fibril[52]; the image above 'Molecular dynamics (MD)' depicts a molecular dynamics model[52]; the inlay above 'Density functional theory (DFT)' shows a snapshot of a molecular simulation of an Alzheimer's β-amyloid peptide oligomer (reproduced with permission from ref. 48, © 2002 NAS); and the image below 'Continuum models' shows a finite element model of an amyloid fibril (reproduced with permission from ref. 25, © 2005 ACS). Bottom panel: Hierarchical structure in linguistics as an analogy to demonstrate how functional properties emerge owing to the hierarchical assembly of simple building blocks. Figures in the bottom panel reproduced with permission from ref. 103, © 2007 Random House.

On the nanoscale, because elastic energy associated with small strain deformation becomes comparable to the thermal energy, spontaneous fluctuations of the fibril shape can occur and the statistical analysis of these geometric fluctuations can be used to measure mechanical properties[29,30]. Such an analysis has been carried out for different amyloid fibril systems and yields an E range of 0.2–14 GPa[31,32]. Further methods, including high-pressure X-ray diffraction studies[33] and statistical analysis of electron microscopy images of individual fibrils[34] show that amyloid fibrils commonly possess an elastic modulus in or close to the GPa range (Fig. 3).

This fluctuation analysis approach to nanomechanical characterization is advantageous over direct mechanical manipulation because fluctuations are evaluated on a length scale that greatly exceeds the tip radius; knowledge of the size or shape of the AFM tip is not required to interpret the measured data. However, the presence of a surface or of interactions between individual structures has the potential to lead to fluctuations other than those given by simple thermal motion of individual fibrils, and can represent an experimental challenge[35].

Figure 3a summarizes the bending rigidity versus moment of inertia for covalent materials (the orange region), strong

Table 1 | Summary of key terms related to amyloid materials science and nanotechnology.

Term/concept	Definition	Relevance for amyloid and/or context, example	Nanotechnology relevance and/or potential applications
Cross-β structure	Basic structural motif of amyloid fibrils consisting of β-strands oriented perpendicular to the fibril axis.	Responsible for many of the nanoscale characteristics of amyloid fibrils, including their high elastic modulus.	Generic structural motif, mechanically and chemically stable owing to high density of H-bond clusters.
Amyloid fibril or fibre	Stack of cross-β motifs to form an elongated nanostructure. Diameters: typically 2–15 nm; length: typically 0.5–10 μm.	Forms the basis for larger-scale assemblies, for example, amyloid plaques; see Fig. 1 or Fig. 5 for illustration.	Provides the basis for patterning constituents that do not form organized nanostructures on their own, such as metal particles or biochemically active agents (examples shown in Fig. 3b–h).
Amyloid plaques and biofilms	Micro to macroscale deposits of amyloid material in tissue, for example, the brain in Alzheimer's disease or in bacterial biofilms.	Assemblies of amyloid fibres; see Fig. 1 for several examples.	Control of patterning of amyloid fibrils in artificial films or on a surface enables the realization of different functional properties (Fig. 5a), for example, coatings, optical and electrical.
Prion	Proteinaceous particle responsible for the transmission of infectious conditions.	Prions propagate by transmitting a misfolded protein state (an amyloid structure in the case of yeast and probably a structurally related molecular species in the case of mammalian prions).	Design of self-replicating systems based on proteins and peptides.
Prionoid	General class of self-propagating protein elements but that lack microbiological transmissibility.	Many amyloid fibril systems have the ability to act as prionoids.	Self-regenerating and self-healing materials.
Strains	Classes of amyloid structures formed from polypeptide chains with an identical sequence but possessing a different three-dimensional packing.	Structural basis for the propagation of amyloid forms with different properties formed from a given protein.	Capacity to change functional properties of a material by assembling into different structures based on the same building blocks.
Mutability, tunability	Capacity to change functional properties of a material based on external signals (pH, light, for instance); in contrast to tunability, which is the capacity to change material reversibly during use.	Spontaneous growth of amyloid plaques in the context of disease states leading to changes in the properties of tissues.	Multifunctional materials with switchable states, for example, substrate patterning for tissue engineering, nanoscale valves and switches.
Optimality	Adaptation to reach a desired characteristic while respecting a set of restrictions.	Maximal stiffness of protein materials based on weak non-covalent bonding (performance limit), see Fig. 3.	Design of stiff materials based on peptide and protein constituents.
Evolvability	Ability to acquire new functions or features in response to changed conditions.	Self-replicating mechanisms associated with prion disease.	Design of self-adaptive materials, autonomous systems.
Universality	Occurrence of structure or mechanism (generally: protocol) in a great variety of systems.	Universal features in amyloid materials include cross-β structure, hydrogen bonding, fibrillar nature and uniform diameter.	Universality of constituents underlies the ability to serve as generic building blocks.
Diversity	Occurrence of structure or mechanism in many guises, commonly linked to a particular functionality.	Diverse features in amyloid materials including sequence-dependent chemical nature of the side chains.	Use of diverse hierarchical structures enables the development of functional properties unique to a particular system (Fig. 5a) despite the presence of few universal building blocks (universality–diversity–paradigm).

non-covalent interactions (blue region) and weak non-covalent interactions (green region). The relationship of amyloid structures to these general material classes can be seen from the blue points that represent amyloid fibrils (different symbols denote data from different studies) and grey symbols are other materials[25,31–34,36–38] shown for comparison. In some cases where the *E* value of amyloid fibrils has been probed in the direction perpendicular to the fibril axis, significantly lower values have been reported (grey inverted triangles in Fig. 3a)[39]. This indicates a high level of anisotropy, and the lateral mechanical response is likely to be highly sensitive to the interactions between the component protofilaments rather than defined primarily through the intrinsic interactions within the β-sheet-rich amyloid core.

Measurements of the nanomechanics of less ordered forms of amyloid structures, known as protofibrillar assemblies, show[35,38] that they possess a lower value of *E* compared with mature amyloid fibrils, indicating a different level of molecular organization in their core structure. Further detailed analysis of the shape fluctuations of protofibrillar assemblies indicate that heterogeneous populations can exist even within the same species[38]. This fact may be a manifestation of the general tendency of amyloid materials towards polymorphism through the existence of many strains of fibrils formed by the same polypeptide sequence but characterized by subtle changes in the molecular packing of the chains within the fibrils[4,40,41]. Even small changes in the conditions during fibril growth can bias the system towards the formation of a different strain. Examples include quiescent versus agitated incubation conditions[38], the presence of cosolvents[42] and temperature[41]. The structural features that are characteristic of a specific strain are in many cases transmitted to a new generation of fibrils that are grown when a monomeric solution of the protein is exposed to preformed seed fibrils of a given strain. Such strains can in many cases[41] be distinguished through

Table 2 | Examples of different forms of amyloid material (adapted from ref. 70).

Context/function	Protein	Primary localization or organism
Functional amyloid		
Control of transcription	Ure2p	Yeast
Control of translational termination	Sup35	Yeast
Biofilm production	Curlin	E. coli bacteria
Heterkaryon incompatibility	Het-S	Fungi
Pituitary secretory granules	Secretory hormones	Pituitary gland
Melanin biosynthesis	Pmel17	Melanosomes in mammalian skin
Pathological amyloid		
Alzheimer's disease	Amyloid-β (aβ) peptide	Extracellular (central nervous system (CNS))
Parkinson's disease	α-synuclein	Intracellular (CNS)
Taupathies, Alzheimer's diease	Tau protein	Intracellular (CNS)
Systemic amyloidosis	Lysozyme, transthyretin, serum amyloid A, immunoglobulin light chain and others	Various tissues, including liver, heart, spleen, and kidney
Haemodialysis-associated amyloidosis	β2-microglobulin	Various tissues, joints
Prion diseases	Prion protein	Extracellular (CNS)
Huntington's disease	Polyglutamine-rich proteins	Intracellular (CNS)
Type II diabetes	Amylin	Extracellular (pancreas)

their mechanical properties, but a remarkable discriminatory power between even subtle changes in structure in amyloid materials can be achieved through the use of recently developed conjugated polyelectrolytes[43], which possess conformation-dependent fluorescence spectra when bound to amyloid fibrils.

General trends that underlie the modulation of the material properties of amyloid fibrils can be identified. For instance, the highest E values are observed for short peptides such as diphenylalanine (two residues)[25], yeast prion fragment (seven residues) and transthyretin fragment (eleven residues)[32], whereas the lower values tend to be observed for fibrils from longer sequences such as α-lactoglobulin, β-lactalbumin[32] and HypF[38] (Fig. 3). These observations point towards the role of increasing structural disorder arising from the constraints accompanying the packing of increasingly long polypeptides into fibrillar structures; where such effects lead to a less effective search for strong intermolecular bonding, a lower modulus can result. Similar observations have been made on larger scales, where computation studies show that highly organized assemblies of short amyloid fibrils have a larger modulus than less organized superstructures composed of longer amyloid fibrils[44].

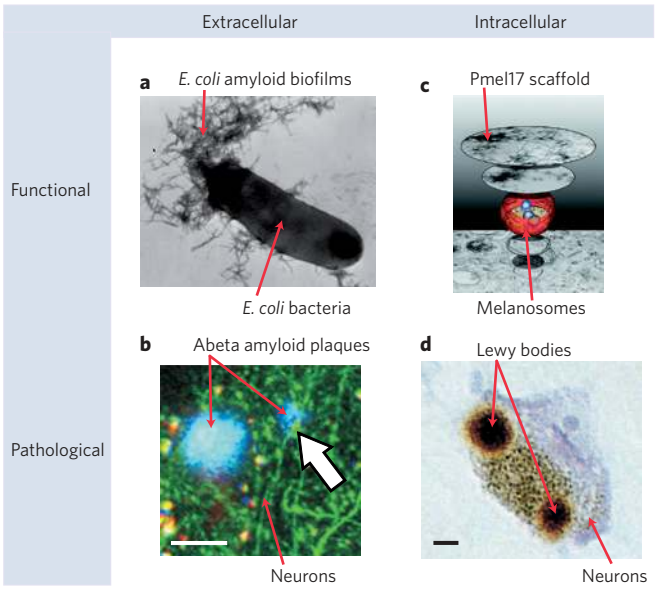

Figure 2 | Classification of amyloid materials. Amyloid materials can be extracellular (**a**,**b**) or intracellular (**c**,**d**), and functional (**a**,**c**) or pathological (**b**,**d**). **a**, Functional amyloid[79] in biofilms produced by bacterial species such as *E. coli* and certain *Salmonella* spp. **b**, Amyloid plaques as seen in a mouse model of Alzheimer's disease (scale bar, 20 μm). The large white arrow shows a newly formed plaque. **c**, Transmission electron microscope image of Pmel17 scaffolds in melanosomes involved in the biosynthesis of melanin. **d**, Lewy bodies, pathological protein aggregates that develop in neurons in Parkinson's disease (scale bar, 8 μm). Figures reproduced with permission from: **a**, ref. 79, © 2007 NAS; **b**, ref. 77, © 2008 NPG; **c**, ref. 20, © 2009 ASBMB; **d**, ref. 21, © 1997 NPG.

The mechanical failure of amyloid materials is at present less well characterized than their linear and elastic deformation at small strain. Experimental values have been obtained from destructive mechanical testing of fibrils using AFM and from the observation of filament fragmentation owing to solvent-imposed shear fields. These measurements yield estimates for the tensile strength of insulin amyloid filaments in the range of 0.1–1 GPa[28,45].

In silico models of amyloid materials have developed into powerful tools to complement experimental methods from first principles. Suitable computational methods include quantum mechanical[46], molecular dynamics[11,13,36,37,47–49], coarse-grained[44,50–53] and continuum approaches[25,52]. A key focus of computational modelling has been the identification of molecular details of the initial stages of amyloid aggregation and defining the nanomechanics of amyloid materials. *In silico* studies of amyloid nanomechanics indicate that the values of E are high for non-covalent materials, in the range of 10–20 GPa, and originate largely from the dense backbone hydrogen-bonding network that extends throughout the core of the structures[35,37,54]. Interactions between groups in the side chains of the polypeptide molecule can further modulate the mechanical properties of the resulting fibrils. This is particularly apparent in cases where side chains can significantly contribute to the hydrogen-bonding patterns, such as in the case of yeast prion fragments[35]. In addition to interactions within the sheets, side-chain interactions play a crucial role in the interactions between the sheets; these interactions typically take the form of a steric zipper, where the complementarity of the adjacent interfaces drives their lateral association[4].

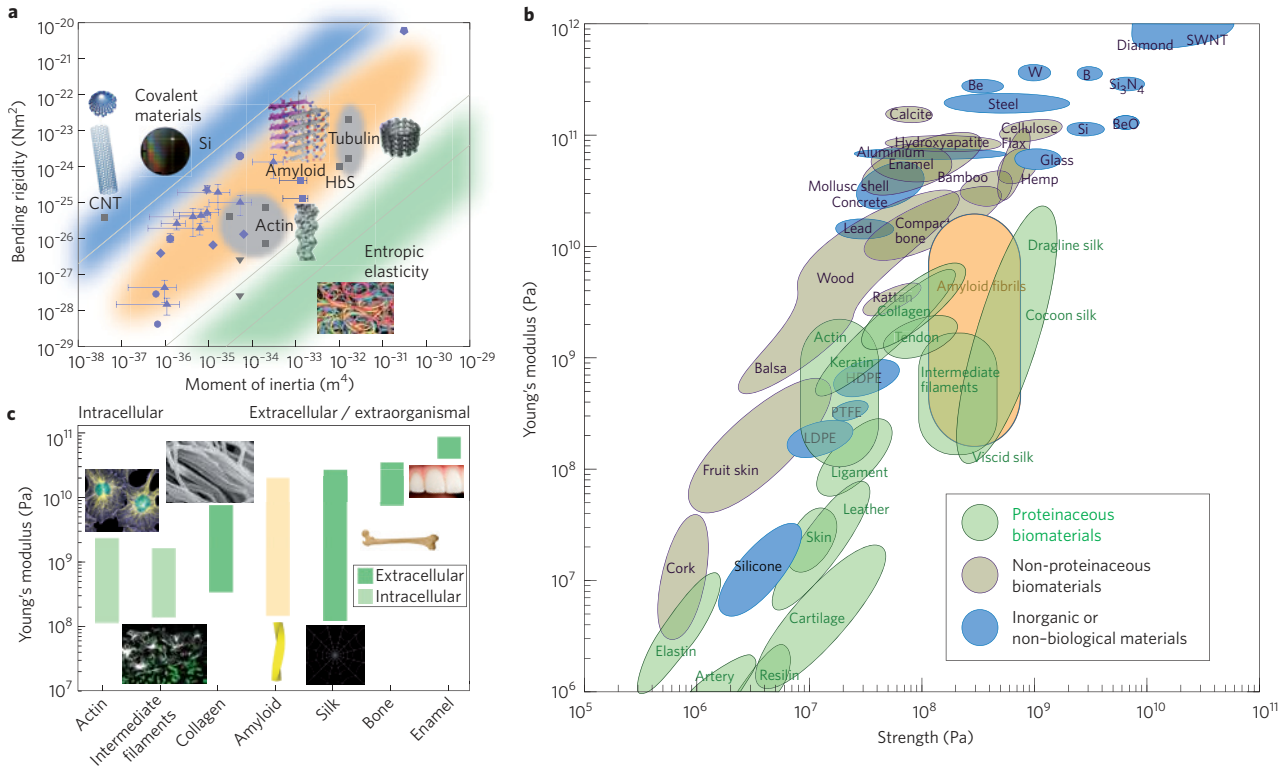

Figure 3 | Mechanical properties of amyloid fibrils in comparison to biological and inorganic or non-biological materials. a, Bending rigidity versus moment of inertia for covalent materials (blue region), strong non-covalent interactions (such as hydrogen bonds, orange region) and weak non-covalent interactions (green region). Blue points are amyloid fibrils (different symbols denote data from different studies) and grey symbols are other materials[25,31–34,36–38]. Grey inverted triangles show the values for the response measured in the perpendicular direction to the fibril axis[39]. The upward triangles show data for one- and two-filament forms of bovine insulin, B-chain of bovine insulin, hen-egg-white lysozyme, bovine β-lactoglobulin, Alzheimer's amyloid β-peptide residues 1-42, GNNQQNY fragment of the yeast prion sup35, and human transthyretin residues 105-115 (all experimental)[32]. The pentagons show data for diphenylalanine (experimental)[25], octagons for insulin (experimental)[33], hexagons for ac-[RARADADA]2-am self-assembling peptide (simulation)[36], stars for Alzheimer's amyloid β-peptide residues 1-40 (simulation)[37], and lozenges show data for β-lactoglobulin (experimental)[31]. The circles show data for the N-terminal domain of the hydrogenase maturation factor HypF (experimental)[38], and squares show data for Alzheimer's amyloid β-peptide residues 1–40 (experimental)[34]. Figures reproduced with permission from: amyloid, ref. 104, © 2005 NPG; actin, ref. 105, © 2008 NAS; tubulin, ref. 106, © 2002 Elsevier. Images courtesy of: silicon wafer © istockphoto.com/photomick; elastic bands © istockphoto.com/shank/-ali. **b**, *E* (which corresponds to stiffness) versus strength[56,57] for a range of different materials. Covalent and metallic bonding results in the stiffest and strongest materials, with diamond and single-wall carbon nanotubes (SWNTs) being the best performers. Silks are the strongest and stiffest protein materials, followed by amyloid and collagen; and significantly more-rigid materials (for example, bone) contain minerals. Amyloid fibrils are shown in orange to distinguish them from other materials. **c**, Range of values of *E* for seven different classes of biological materials inside and outside the cell. The stiffest materials (such as collagen, bone, enamel and silk) are found outside the cell. Images courtesy of: actin © NIGMS/Torsten Wittmann; intermediate filaments © NIGMS/Evan Zamir; collagen © fei.com/Paul Gunning; silk © istockphoto.com/blackjack3d; bone © istockphoto.com/dwithers; enamel © istockphoto.com/shironosov.

Relation to other biological materials

The mechanical properties of materials intimately reflect the nature of the fundamental intermolecular interactions that bind their constituents into larger-scale hierarchical systems. In amyloid materials this connection offers general insights into the characteristics of interactions in natural or artificial proteinaceous materials. Amyloid fibrils can be seen to form a reference class of structures where the core of fibrils consists of arrays of β-strands that involve essentially every residue in the core domain, resulting in continuous β-sheets that can extend over thousands of molecular units, a unique situation in biological materials.

Many amyloid fibrils, especially those formed from proteins that do not undergo assembly towards the amyloidogenic state in nature, have not been directly influenced by evolutionary pressures. As such, these proteins give access to the inherent mechanical properties of β-sheets on supramolecular length scales without the influence of evolutionary adaptation that typically pervades the properties of natural protein materials. Compared with other biological materials (Fig. 3)[55–57], amyloid fibrils are remarkably stiff and possess values of *E* comparable to the most rigid proteinaceous materials in nature. Dragline silk, for example, has a value of *E* of up to 10 GPa, and collagen and keratin both exhibit *E* values approaching this value (Fig. 3b)[45,58–60]. Dragline silk has similarities from a structural point of view with amyloid fibrils, and the crystalline regions of silk[61,62], which contribute to its high *E* value, consist of densely packed hydrogen-bonded β-strands analogous in many ways to those found in the core of amyloid materials.

Considerations based on the maximal density of intermolecular hydrogen bonds that can be achieved in proteins yield a limit for the material performance of proteinaceous structures in terms of *E* on the order of 10–20 GPa[24,32]. In agreement with this concept, materials that posses *E* values significantly above this limit contain covalent or metallic interactions with a significantly higher energy density than hydrogen bonds or similarly weak non-covalent interactions[55].

Nature has therefore, through the action of evolutionary processes, been able to optimize proteinaceous materials to be close to

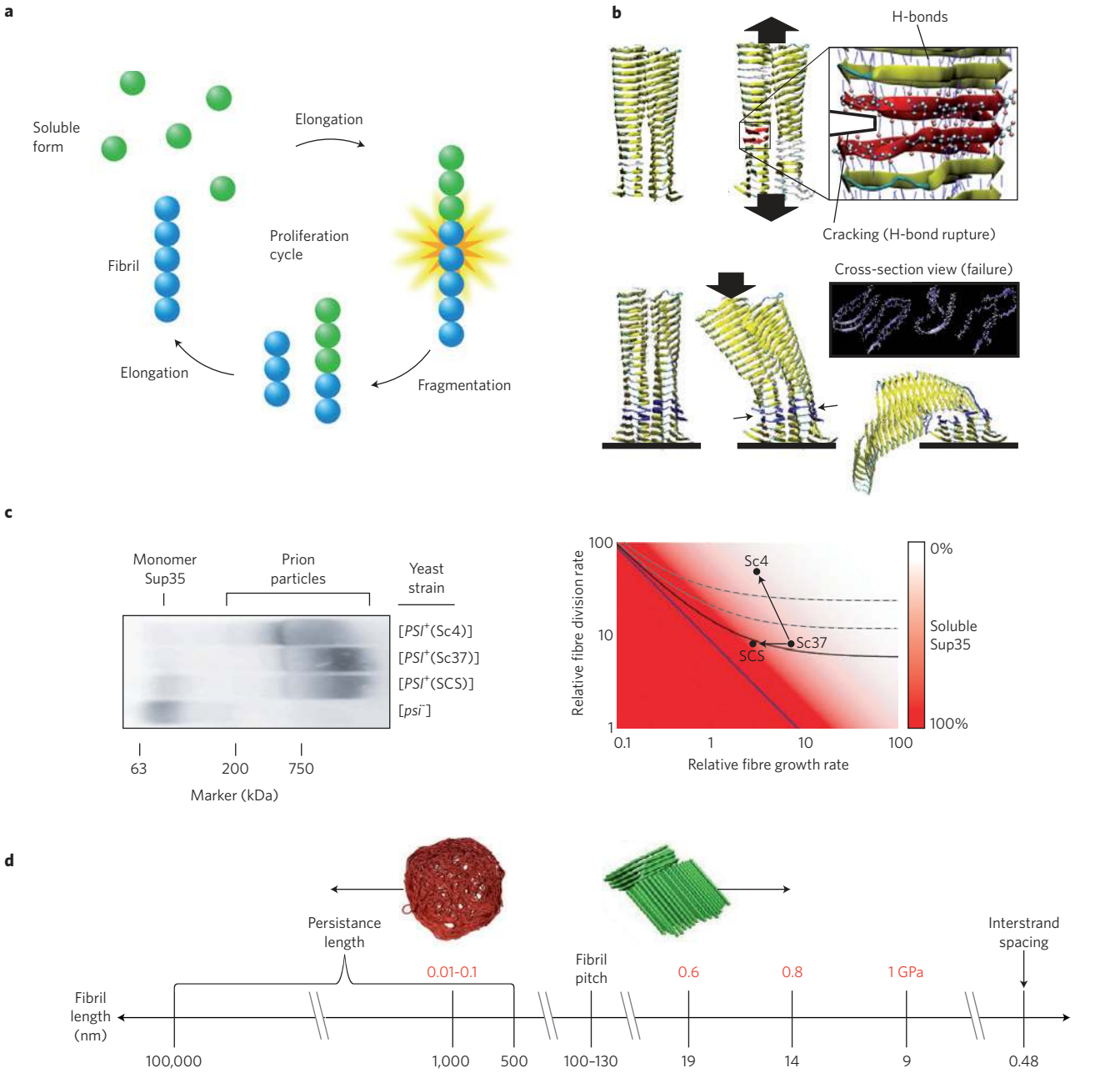

Figure 4 | Fragmentation, aggregation and the kinetics of amyloid growth. a, Schematic illustrating the formation of amyloid fibrils from soluble monomers. On fragmentation, newly formed ends of amyloid fragments serve as seeds for further elongation, and the process repeats[63]. **b**, Molecular mechanism of fragmentation of the cross-β core of amyloid fibrils[65]. Upper part: failure owing to tension, through the opening of a crack due to the breaking of hydrogen bonds. Lower part: failure under compression owing to fluid shear forces or thermal vibrations that excite bending or stretching modes. **c**, Studies of the propagation of three strains of yeast prion (Sc4, Sc37 and SCS) show that there exists an intimate connection between mechanics and the growth kinetics of prion aggregates. These amyloid fibrils formed from the protein Sup35 propagate most effectively in yeast cells in cases where their intrinsic fragmentation rate was high and the mechanical strength correspondingly low. The gel electrophoretic analysis of prion particle size (**c**, left) shows that the greater frangibility of Sc4 fibrils results in a smaller size distribution of the aggregates, but more effective overall growth and sequestering of the monomer relative to the less frangible SCS fibrils. The [*psi*-] case represents a control system with no aggregates. The right panel shows the differences in the fibril breakage rates and growth rates. Reproduced from ref. 41, © 2006 NPG. **d**, The tensile strength in GPa (red numbers, results from computational modelling) of amyloid fibrils of various lengths (black numbers): it can be seen that longer fibrils are weaker[64]. The plot also summarizes characteristic length scales of amyloid fibrils, including the layer spacing (distance between β-sheet layers in the core), the helical pitch in the twisted geometry of the fibrils, and the persistence length (data shown here are for Alzheimer's β-amyloid fibril). As the length of the amyloid fibrils that assemble into plaques is varied, the structure of the assembled plaques changes from being highly organized and regular (green, right) to more entangled and randomized (red, left)[14,28,35,44,65]. This is because of the competition between bending and interfibril adhesion; in shorter fibrils the interfibril adhesion forces are strong enough to align fibrils in parallel, whereas for longer fibrils the entangled arrangement is stable.

the theoretical performance limits. It is apparent, however, that the rigidity of cytoskeletal filaments[57–64] does not extend up to the maximal values achievable for biological materials (Fig. 3c). Intracellular materials are subject to an additional requirement that assembly must be readily reversible under physiological conditions to ensure cellular motility and compatibility with the intracellular environment. Indeed, the strong intermolecular bonding in the materials that exhibit the highest moduli — cellulose, bone, keratin, silk — seems to be incompatible with rapid and dynamic disassembly characteristic of functional intracellular structures, and these materials are primarily found extracellularly and in roles where controlled rapid breakdown is not required.

Failure is the key to growth

The interplay between nanomechanics of amyloid fibrils and their growth kinetics is increasingly appearing as a key factor for the overall conversion of proteins from their soluble to fibrillar states in many amyloid-related phenomena, including the transmission of prions[41,63]. This surprising connection emerges through the importance of filament fragmentation as one of the fundamental factors controlling the proliferation of amyloid fibrils. Because the growth of such structures occurs by addition of soluble proteins to fibril ends, the number of free ends effectively governs the overall conversion reaction (Fig. 4). In agreement with this concept, even small shear forces, which favour fragmentation of filaments but are likely to leave other system parameters largely invariant, are generally observed to significantly accelerate amyloid growth. Despite the substantial strength of amyloid structures, as their length increases through growth, the possibility of structures fragmenting either spontaneously through thermal fluctuation or through the action of cellular agents becomes increasingly likely[64]. Indeed, *in silico* studies of amyloid fibril failure suggested that longer fibrils are more brittle elements that show a greater propensity towards failure as their length increases (Fig. 4d)[24,65].

The role of fragmentation is particularly marked for prion-type aggregates. These aggregates are characterized by their remarkable ability to proliferate and infect organisms where the soluble, non-aggregated form of the prion protein is available[66]. Examples of such behaviour are known in a variety of organisms including fungi and mammals. For this class of structure, the spontaneous generation of new fibrils through primary nucleation is generally very slow, and secondary pathways such as fragmentation are therefore critical in generating new growth sites as the reaction progresses (Fig. 4c)[63]. Amyloid fibrils formed from the yeast protein Sup35 were shown to propagate as prions most effectively in yeast cells in cases where their intrinsic fragmentation rate was high and the mechanical strength correspondingly low[41,65]. Although mammalian prion systems are more complex than their yeast analogues, trends indicative of a similar connection have been identified. Indeed, the time before disease development in a mouse model of prion disease was found to be inversely correlated with the aggregate stability. This suggests a lower stability contributing to a higher fragmentation rate, more effective prion proliferation and thus a more rapid onset of disease symptoms[67].

Interestingly, recent evidence points towards remarkable underlying similarities between prion conditions and other amyloid disorders such as Alzheimer's disease[66,68,69]. Indeed, although under most circumstances true infection between organisms remains confined to prion type aggregates, it has been demonstrated that amyloid fibrils formed from many other proteins can also be released from cells where they have grown and can infect neighbouring cells, giving rise to the concept of a prionoid as a general self-propagating protein element[66,70].The role of material failure therefore, shown to be crucial in the proliferation of prions as discussed above, may also be important in the development of other amyloid pathologies. Furthermore, many recent studies suggest that the deleterious activity associated with protein aggregates stems from aggregates of small molecular weight. Although their source has still to be established with certainty, it could be hypothesized that their release from larger plaques to form a halo of small oligomers[71] through fragmentation may be a significant contribution[72].

Natural uses of amyloid as a functional material

Ever since their discovery, amyloid fibrils have been primarily associated with pathological behaviour[10,12]; but amyloid structures are in fact also naturally found in many functional roles[15,16,18,19,73,74]. Prominent examples of such functional amyloid materials include bacterial coatings[75], catalytic scaffolds[16], agents mediating epigenetic-information storage and transfer[76], adhesives[19] and structures for the storage of peptide hormones[74]. The existence of functional amyloid is highly significant, because it demonstrates that the amyloid fold is not unequivocally connected to toxicity and disease[8,10,77]. Rather, it represents a more general ordered state for proteins that is often energetically favourable compared with the soluble native state[1]. These discoveries are remarkable from a biological point of view as they highlight the delicate distinction between pathology and physiology, but they are also intriguing because they point to the possibility of using amyloid as a powerful platform for the design of new nanomaterials.

Functional amyloid was initially identified in single-cell organisms. Many such applications are characterized by the use of amyloid as a structural material. Bacteria, including *Escherichia coli* (*E. coli*), use an extracellular amyloid material, curli fibres, as the basis for generating a matrix for surface adhesion and interactions with other bacteria (Fig. 2a)[75,78,79]. Several species of fungi, including the common baker's yeast, use amyloid fibrils for storing epigenetic information. Here amyloid structures implement a switch, the state of which is defined through the presence of an amyloidogenic protein either in its soluble or fibrillar form. Aggregates in the cytoplasm will be transmitted to the daughter cells during cell division; when aggregates are present they will act as seeds to promote the conversion of the relevant protein into its fibrillar state also in the daughter cells, and conversely when no aggregates are present in the mother cell, the amyloid conversion is significantly less likely. The information encoded directly through the bistability in the configuration of a protein is therefore inheritable. Another natural use of amyloid as a functional material is as a component of extracellular polymeric substances secreted by algae that mediate surface adhesion[19].

Functional amyloid is not a phenomenon restricted to single-cell organisms. Indeed, an example of amyloid scaffolds possessing a key physiological role has emerged in the biosynthesis of melanin in humans[16]. Melanin synthesis in melanosomes, specialized secretory organelles in melanocytes in the skin and eyes, occurs through polymerization of small molecule precursors. This process is catalysed by a scaffold of amyloid fibrils formed from the protein Pmel17 (refs 18,20; Fig. 2c). The role of the amyloid scaffold is thought to be related to a templating process, where the effective concentration of precursor molecules is increased through their adsorption onto the catalytical scaffold. The efficiency of the reaction may be enhanced through the orientational preference provided by amyloid fibrils. Amyloid fibrils may have many other functional roles in mammalian systems, and recently a further natural application was revealed in the form of high-density packing of peptide hormones in the secretory granules in pituitary glands[74]. Here the formation of amyloid fibrils helps to isolate peptides with a given sequence as well as stabilize the hormones during storage before secretion.

The amyloid fold can provide an effective basis for the formation of robust fibrillar materials through self-assembly. A key open question is the lack of toxicity to the host organism synthesizing functional amyloid when compared with the deleterious effects associated with the deposition of amyloid in disease states. Some insights that could resolve this paradox come from the realization that the formation of functional amyloid is frequently under tight

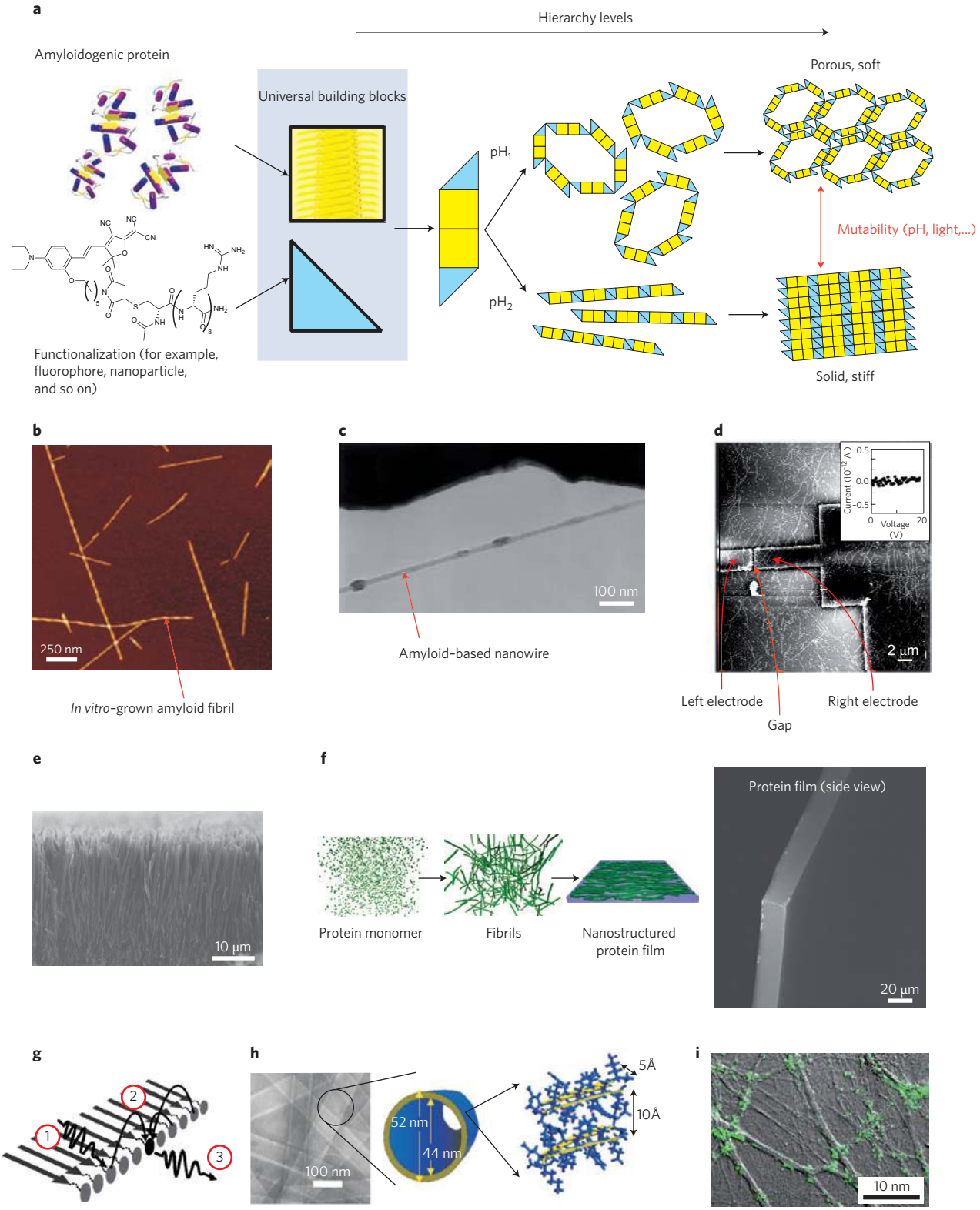

Figure 5 | Examples of functional synthetic amyloid materials. a, Amyloid formation from a native protein results in universal building blocks that can be assembled and functionalized (for example, with fluorophores or metal particles) into larger and more diverse structures. Different structures can be achieved through changes in pH or other processing conditions. **b**, AFM image of synthetic amyloid fibrils generated *in vitro*[35]. **c**–**f**, The fibrils can assemble to form conducting nanowires (**c**,**d**)[86,88], surface coatings (**e**)[91] and nanostructured protein films (**f**)[93]. **g**, Schematic showing a light-harvesting nanostructure generated from amyloid fibrils[95]. Light harvesting occurs by means of absorption of a photon by the donor (1), followed by non-emissive transfer to an acceptor through resonance energy transfer (2). The energy is released by the acceptor as a photon (3). **h**, Hollow nanotubes made from amyloid structures could be used to develop new nanoscale antenna[96]. **i**, Optical image of active neuron synapses (labelled with a green fluorescent lipophilic probe) whose growth was stimulated by β-sheet-rich scaffolds[98]. Figure reproduced with permission from: **b**, ref. 35, © 2007 AAAS; **c**, ref. 86, © 2006 ACS; **d**, ref. 88, © 2003 NAS; **e**, ref. 91, © 2009 NPG; **f**, ref. 93, © 2010 NPG; **g**, ref. 95, © 2009 ACS; **h**, ref. 96, © 2008 RSC; **i**, ref. 98, © 2000 NAS.

control and takes place under conditions that favour rapid and effective polymerization[75] such that the formation of potentially toxic low-molecular-weight oligomers or other intermediates is avoided.

Synthetic amyloid-based nanostructures and applications

Multifunctionality in natural proteinaceous materials is usually produced by assembling a few simple (and often lower-performance) elements into structures that are characterized by multiple length-scales (Fig. 5a). This is completely different from the traditional engineering approach, which involves the use of a large number of distinct (and often high-quality) building blocks. An intriguing aspect of amyloid mechanics is the manner by which weak non-covalent intermolecular chemical bonds generate mechanically strong materials. *In silico* studies show that the key to the creation of strength from weak hydrogen bonding is their grouping into clusters, arranged in β-strands with a relatively short length. This universal design feature allows hydrogenbonds to work cooperatively and reach maximum strength[24,83]. Many of the natural applications of amyloid materials discussed above capitalize on their robust properties and readily self-assembling nature in the absence of external energy input such as ATP; these characteristics are also of interest for synthetic biomaterials, and the discovery of functional amyloid has provided the inspiration for the development of artificial amyloid materials.

An advantage of biological self-assembly is the ability to generate and control structure on the nanoscale, as shown schematically in Fig. 5a. This natural propensity for nanoscale organization into fibrils (Fig. 5b)[35,84] can be used to template other materials that do not on their own possess a propensity to form ordered structures on that scale, such as metal particles[85]. This strategy, which arranges universal building blocks into hierarchical structures to create diverse functional materials that are similar to natural materials, offers opportunities in hierarchical *de novo* material design. The power of this principle has been demonstrated in the fabrication of conductive nanowires, where the self-assembling peptide fibrils act as templates for the deposition of metals on the outside of structures to yield electrically conducting wires (Fig. 5c,d)[86–88]. Diphenylalanine nanotubes are of particular interest in this context because these structures contain a hollow core; deposition of metal both within and on the outside of these structures results in coaxial nanowires with electromagnetic properties[89]. The assembly of amyloid fibrils into larger-scale structures also provides the opportunity to realize new surface (Fig. 5e)[90–92] and bulk (Fig. 5f)[93] properties. The propensity of proteins to undergo multilevel hierarchical assembly opens up the possibility of larger-scale structures to be generated through self-assembly, while maintaining the accurate control of nanoscale organization[93].

Another use of amyloid scaffolds has been demonstrated in the context of organic photovoltaics[94]. A challenge in the fabrication of such materials stems from the requirement to generate and control a large interfacial area between electron donor and acceptor materials where photocharges are created. Improved characteristics were reported for organic solar cells where amyloid fibrils were used as a template to orient the donor and acceptor polymers and to enhance the area of the donor–acceptor interface. The assembly of a peptide scaffold can also be used to drive the organization of host species attached to the peptides before assembly. This has enabled the creation of linear nanoscale arrays of fluorescent species that on illumination allow energy migration along the scaffold in the form of eximers. When binary structures are created that include both acceptor and donor groups in the same fibril scaffold, excitation of donor species by incident light allows energy transfer to acceptor sites where the energy can be converted back to light, and emission can be observed. Such structures can operate as light-harvesting materials (Fig. 5g)[95]. A recent study demonstrated the assembly of strong chromophores (colouring pigments) across a paracrystalline amyloid network, which allows for precise ordering along the inner and outer compartment walls of an amyloid-based protein nanotube in a nanoscale antenna[96] (Fig. 5h).

The inherently fibrillar nature of amyloid materials alone can lead to useful modifications to the chemical availability of biologically active species. In particular, amyloid has been explored for controlled-release drug delivery, where longer-lasting action can be achieved through the slow dissociation of peptide nanostructures after administration. This principle has been demonstrated in the context of cancer therapy, based on, for example, gonadotropin-releasing hormone, the action of which can be significantly prolonged when fibrillar rather then monomeric material is administered[97]. The fibrillar structures of amyloid materials are also applied in three-dimensional tissue-culture scaffold design[98] (Fig. 5i), for brain repair through axon regeneration[99], or for the modulation of cell adhesion[100].

The paradigm of using hierarchical structures to create diversity of function out of simple, universal elements, as seen in amyloid nanomaterials, is in many ways analogous to linguistics (Fig. 1)[101]; a set of letters of the alphabet are used to form words, which are assembled into sentences, which are assembled into paragraphs, chapters and eventually an entire book. The construction of language exemplifies how the interplay of diversity and universality provide a powerful bottom-up design approach that can be applied to the development of nanomaterials (see Fig. 5).

Conclusion

The nanoscale mechanics of amyloid fibrils underlies many aspects of the behaviour of these materials in their different biological contexts, including molecular medicine, biomechanics and functional bionanomaterials. Understanding the role of nanoscale-material failure in the fragmentation of aggregates and the proliferation of amyloid fibrils in prion and related disorders offers insights into the structural and mechanistic differences between physiologically useful and pathological amyloid structures. The principle of hierarchical assembly in the amyloid scaffold can potentially be exploited to generate new forms of functional biomaterials with a wide range of physical properties in which a small number of abundant natural building blocks assemble to yield high-performance but environmentally benign materials.

References

1. Dobson, C. M. Protein misfolding, evolution and disease. *Trends Biochem. Sci.* **24,** 329–32 (1999).
2. Jaroniec, C. P. *et al.* High-resolution molecular structure of a peptide in an amyloid fibril determined by magic angle spinning NMR spectroscopy. *Proc. Natl Acad. Sci.USA* **101,** 711–716 (2004).
3. Luhrs, T. *et al.* 3D structure of Alzheimer's amyloid-beta(1–42) fibrils. *Proc. Natl Acad. Sci.USA* **102,** 17342–17347 (2005).
4. Sawaya, M. R. *et al.* Atomic structures of amyloid cross-beta spines reveal varied steric zippers. *Nature* **447,** 453–457 (2007).
5. Wasmer, C. *et al.* Amyloid fibrils of the HET-s(218–289) prion form a beta solenoid with a triangular hydrophobic core. *Science* **319,** 1523–1526 (2008).

Refs 2–5: structures of the amyloid cross-beta motifs illustrate many of the key characteristics of amyloid materials in atomic detail.

6. Sipe, J. D. & Cohen, A. S. Review: History of the amyloid fibril. *J. Struct. Biol.* **130,** 88–98 (2000).
7. Tan, S. Y. & Pepys, M. B. Amyloidosis. *Histopathology* **25,** 403–414 (1994).
8. Selkoe, D. J. Alzheimer's disease: Genes, proteins, and therapy. *Physiol. Rev.* **81,** 741–766 (2001).
9. Antzutkin, O. N. *et al.* Multiple quantum solid-state NMR indicates a parallel, not antiparallel, organization of beta-sheets in Alzheimer's beta-amyloid fibrils. *Proc. Natl Acad. Sci.USA* **97,** 13045–13050 (2000).
10. Bucciantini, M. *et al.* Inherent toxicity of aggregates implies a common mechanism for protein misfolding diseases. *Nature* **416,** 507–511 (2002).
11. Tsai, H. H. *et al.* Energy landscape of amyloidogenic peptide oligomerization by parallel-tempering molecular dynamics simulation: significant role of Asn ladder. *Proc. Natl Acad. Sci. USA* **102,** 8174–8179 (2005).
12. Pepys, M. B. Amyloidosis. *Ann. Rev. Med.* **57,** 223–241 (2006).

13. Zanuy, D., Gunasekaran, K., Lesk, A. M. & Nussinov, R. Computational study of the fibril organization of polyglutamine repeats reveals a common motif identified in beta-helices. *J. Mol. Biol.* **358,** 330–45 (2006).
14. Paravastu, A. K., Leapman, R. D., Yau, W. M. & Tycko, R. Molecular structural basis for polymorphism in Alzheimer's beta-amyloid fibrils. *Proc. Natl Acad. Sci.USA* **105,** 18349–18354 (2008).
15. Chiti, F. & Dobson, C. M. Protein misfolding, functional amyloid, and human disease. *Annu. Rev. Biochem.* **75,** 333–66 (2006).
Overview of the principles of protein folding and misfolding.
16. Fowler, D. M. *et al.* Functional amyloid formation within mammalian tissue. *PLoS Biol.* **4**, e6 (2006).
Functional amyloid in the synthesis of melanin.
17. Fowler, D. M., Koulov, A. V., Balch, W. E. & Kelly, J. W. Functional amyloid-from bacteria to humans. *Trends Biochem. Sci.* **32,** 217–24 (2007).
18. Kelly, J. W. & Balch, W. E. Amyloid as a natural product. *J. Cell Biol.* **161,** 461–462 (2003).
19. Mostaert, A. S., Higgins, M. J., Fukuma, T., Rindi, F. & Jarvis, S. P. Nanoscale mechanical characterisation of amyloid fibrils discovered in a natural adhesive. *J. Biol. Phys.* **32,** 393–401 (2006).
20. Watt, B. *et al.* N-terminal domains elicit formation of functional Pmel17 amyloid fibrils. *J. Biol. Chem.* **284,** 35543–35555 (2009).
21. Spillantini, M. G. *et al.* α-Synuclein in Lewy bodies. *Nature* **388,** 839–840 (1997).
22. Fandrich, M., Fletcher, M. A. & Dobson, C. M. Amyloid fibrils from muscle myoglobin. *Nature* **410,** 165–166 (2001).
23. Dobson, C. M. Protein folding and misfolding. *Nature* **426,** 884–90 (2003).
24. Keten, S., Xu, Z., Ihle, B. & Buehler, M. J. Nanoconfinement controls stiffness, strength and mechanical toughness of beta-sheet crystals in silk. *Nature Mater.* **9,** 359–367 (2010).
25. Kol, N. *et al.* Self-assembled peptide nanotubes are uniquely rigid bioinspired supramolecular structures. *Nano Lett.* **5,** 1343–1346 (2005).
26. Salvetat, J. P. *et al.* Elastic and shear moduli of single-walled carbon nanotube ropes. *Phys. Rev. Lett.* **82,** 944–947 (1999).
27. Kis, A. *et al.* Nanomechanics of microtubules. *Phys. Rev. Lett.* **89,** 248101 (2002).
28. Smith, J. F., Knowles, T. P. J., Dobson, C. M., MacPhee, C. E. & Welland, M. E. Characterization of the nanoscale properties of individual amyloid fibrils. *Proc. Natl Acad. Sci.USA* **103,** 15806–15811 (2006).
29. Gittes, F., Mickey, B., Nettleton, J. & Howard, J. Flexural rigidity of microtubules and actin-filaments measured from thermal fluctuations in shape. *J. Cell Biol.* **120,** 923–934 (1993).
30. Wang, J. C. *et al.* Micromechanics of isolated sickle cell hemoglobin fibers: Bending moduli and persistence lengths. *J. Mol. Biol.* **315,** 601–612 (2002).
31. Adamcik, J. *et al.* Understanding amyloid aggregation by statistical analysis of atomic force microscopy images. *Nature Nanotech.* **5,** 423–428 (2010).
32. Knowles, T. P. *et al.* An analytical solution to the kinetics of breakable filament assembly. *Science* **326,** 1533–1537 (2009).
33. Meersman, F., Cabrera, R. Q., McMillan, P. F. & Dmitriev, V. Compressibility of insulin amyloid fibrils determined by X-ray diffraction in a diamond anvil cell. *High Pressure Res.* **29,** 665–670 (2009).
34. Sachse, C., Grigorieff, N. & Fandrich, M. Nanoscale flexibility parameters of Alzheimer amyloid fibrils determined by electron cryo-microscopy. *Angew. Chem. Int. Ed.* **49,** 1321–1323 (2010).
35. Knowles, T. P. *et al.* Role of intermolecular forces in defining material properties of protein nanofibrils. *Science* **318,** 1900–1903 (2007).
Determination of the rigidities of nanofibrils formed from a wide range of peptides and proteins.
36. Park, J., Kahng, B., Kamm, R. D. & Hwang, W. Atomistic simulation approach to a continuum description of self-assembled beta-sheet filaments. *Biophys. J.* **90,** 2510–2524 (2006).
37. Paparcone, R., Keten, S. & Buehler, M. J. Atomistic simulation of nanomechanical properties of Alzheimer's A beta(1–40) amyloid fibrils under compressive and tensile loading. *J. Biomechanics* **43,** 1196–1201 (2010).
38. Relini, A. *et al.* Detection of populations of amyloid-like protofibrils with different physical properties. *Biophys. J.* **98,** 1277–1284 (2010).
39. Guo, S. & Akhremitchev, B. B. Packing density and structural heterogeneity of insulin amyloid fibrils measured by AFM nanoindentation. *Biomacromolecules* **7,** 1630–1636 (2006).
40. Petkova, A. T. *et al.* Self-propagating, molecular-level polymorphism in Alzheimer's beta-amyloid fibrils. *Science* **307,** 262–265 (2005).
41. Tanaka, M., Collins, S. R., Toyama, B. H. & Weissman, J. S. The physical basis of how prion conformations determine strain phenotypes. *Nature* **442,** 585–589 (2006).
Role of fibril fragmentation and nanomechanics in the propagation of yeast prion fibrils.
42. Dzwolak, W., Smirnovas, V., Jansen, R. & Winter, R. Insulin forms amyloid in a strain-dependent manner: An FT-IR spectroscopic study. *Protein Sci.* **13,** 1927–1932 (2004).
43. Sigurdson, C. J. *et al.* Prion strain discrimination using luminescent conjugated polymers. *Nature Meth.* **4,** 1023–1030 (2007).
Luminescent conjugated polymers as powerful probes of polymorphism in protein aggregates.
44. Paparcone, R., Cranford, S. W. & Buehler, M. J. Self-folding and aggregation of amyloid fibrils *Nanoscale* **3**, 1748–1755 (2011).
45. Huang, Y. Y., Knowles, T. P. J. & Terentjev, E. M. Strength of nanotubes, filaments, and nanowires from sonication-induced scission. *Adv. Mater.* **21,** 3945–3948 (2009).
46. Streltsov, V. X-ray absorption and diffraction studies of the metal binding sites in amyloid beta-peptide. *Eur. Biophys. J.* **37,** 257–263 (2008).
47. Ackbarow, T., Chen, X., Keten, S. & Buehler, M. J. Hierarchies, multiple energy barriers and robustness govern the fracture mechanics of alpha-helical and beta-sheet protein domains. *Proc. Natl Acad. Sci. USA* **104,** 16410–16415 (2007).
48. Ma, B. & Nussinov, R. Stabilities and conformations of Alzheimer's beta-amyloid peptide oligomers (Abeta 16–22, Abeta 16–35, and Abeta 10–35): Sequence effects. *Proc. Natl Acad. Sci. USA* **99,** 14126–14131 (2002).
49. Periole, X., Rampioni, A., Vendruscolo, M. & Mark, A. E. Factors that affect the degree of twist in beta-sheet structures: a molecular dynamics simulation study of a cross-beta filament of the GNNQQNY peptide. *J. Phys. Chem. B* **113,** 1728–1737 (2009).
50. Lee, C. F., Loken, J., Jean, L. & Vaux, D. J. Elongation dynamics of amyloid fibrils: A rugged energy landscape picture. *Phys. Rev. E* **80,** 041906 (2009).
51. Wei, G. H., Mousseau, N. & Derreumaux, P. Computational simulations of the early steps of protein aggregation. *Prion* **1,** 3–8 (2007).
52. Xu, Z., Paparcone, R. & Buehler, M. J. Alzheimer's abeta(1–40) amyloid fibrils feature size-dependent mechanical properties. *Biophys. J.* **98,** 2053–2062 (2010).
53. Auer, S. *et al.* Importance of metastable states in the free energy landscapes of polypeptide chains. *Phys. Rev. Lett.* **99,** 178104 (2007).
54. Xu, Z. & Buehler, M. J. Mechanical energy transfer and dissipation in fibrous beta-sheet-rich proteins. *Phys. Rev. E* **81,** 061910 (2010).
55. Fratzl, P. & Weinkamer, R. Nature's hierarchical materials. *Prog. Mater. Sci.* **52,** 1263–1334 (2007).
56. Ashby, M. F., Gibson, L. J., Wegst, U. & Olive, R. The mechanical properties of natural materials. I. Material property charts. *Proc. R. Soc. Lond. A* **450,** 123–140 (1995).
57. Wegst, U. G. K. & Ashby, M. F. The mechanical efficiency of natural materials. *Phil. Mag.* **84,** 2167–2181 (2004).
58. Kreplak, L., Bar, H., Leterrier, J. F., Herrmann, H. & Aebi, U. Exploring the mechanical behavior of single intermediate filaments. *J. Mol. Biol.* **354,** 569–577 (2005).
59. Yang, L. *et al.* Micromechanical bending of single collagen fibrils using atomic force microscopy. *J. Biomed. Mater. Res. A* **82,** 160–168 (2007).
60. Shen, Z. L., Dodge, M. R., Kahn, H., Ballarini, R. & Eppell, S. J. Stress-strain experiments on individual collagen fibrils. *Biophys. J.* **95,** 3956–3963 (2008).
61. Slotta, U. *et al.* Spider silk and amyloid fibrils: A structural comparison. *Macromol. Biosci.* **7,** 183–188 (2007).
62. Vollrath, F. & Knight, D. P. Liquid crystalline spinning of spider silk. *Nature* **410,** 541–548 (2001).
63. Collins, S. R., Douglass, A., Vale, R. D. & Weissman, J. S. Mechanism of prion propagation: amyloid growth occurs by monomer addition. *PLoS Biol.* **2**, e321 (2004).
64. Shorter, J. & Lindquist, S. Destruction or potentiation of different prions catalyzed by similar Hsp104 remodeling activities. *Mol. Cell* **23,** 425–438 (2006).
65. Paparcone, R. & Buehler, M. J. Failure of A-beta-(1–40) amyloid fibrils under tensile loading. *Biomaterials* **32,** 3367–3374 (2011).
Molecular mechanisms of failure of amyloid fibrils and influence of fibril length on mechanical properties.
66. Aguzzi, A. Cell biology: Beyond the prion principle. *Nature* **459,** 924–925 (2009).
67. Prusiner, S. B. Molecular biology of prion diseases. *Science* **252,** 1515–1522 (1991).
68. Riek, R. Cell biology: infectious Alzheimer's disease? *Nature* **444,** 429–431 (2006).
69. Eisele, Y. S. *et al.* Peripherally applied A beta-containing inoculates induce cerebral beta-amyloidosis. *Science* **330,** 980–982 (2010).
70. Aguzzi, A. & Rajendran, L. The transcellular spread of cytosolic amyloids, prions, and prionoids. *Neuron* **64,** 783–790 (2009).
71. Koffie, R. M. *et al.* Oligomeric amyloid beta associates with postsynaptic densities and correlates with excitatory synapse loss near senile plaques. *Proc. Natl Acad. Sci. USA* **106,** 4012–4017 (2009).
72. Haass, C. & Selkoe, D. J. Soluble protein oligomers in neurodegeneration: lessons from the Alzheimer's amyloid beta-peptide. *Nature Rev. Mol. Cell Biol.* **8,** 101–112 (2007).
73. Gebbink, M. F. B. G., Claessen, D., Bouma, B., Dijkhuizen, L. & Wosten, H. A. B. Amyloids - A functional coat for microorganisms. *Nature Rev. Microbiol.* **3,** 333–341 (2005).

74. Maji, S. K. *et al.* Functional amyloids as natural storage of peptide hormones in pituitary secretory granules. *Science* **325,** 328–332 (2009).
Discovery of functional amyloid in the endocrine system.
75. Chapman, M. R. *et al.* Role of Escherichia coli curli operons in directing amyloid fiber formation. *Science* **295,** 851–855 (2002).
Involvement of functional amyloid in bacterial biofilm production.
76. Shorter, J. & Lindquist, S. Prions as adaptive conduits of memory and inheritance. *Nature Rev. Genet.* **6,** 435–450 (2005).
77. Meyer-Luehmann, M. *et al.* Rapid appearance and local toxicity of amyloid-beta plaques in a mouse model of Alzheimer's disease. *Nature* **451,** 720–724 (2008).
78. Barnhart, M. M. & Chapman, M. R. Curli biogenesis and function. *Annu. Rev. Microbiol.* **60,** 131–147 (2006).
79. Hammer, N. D., Schmidt, J. C. & Chapman, M. R. The curli nucleator protein, CsgB, contains an amyloidogenic domain that directs CsgA polymerization. *Proc. Natl Acad. Sci. USA* **104,** 12494–12499 (2007).
80. Zhang, S. G., Holmes, T., Lockshin, C. & Rich, A. Spontaneous assembly of a self-complementary oligopeptide to form a stable macroscopic membrane. *Proc. Natl Acad. Sci. USA* **90,** 3334–3338 (1993).
81. Zhang, S. G. Fabrication of novel biomaterials through molecular self-assembly. *Nature Biotechnol.* **21,** 1171–1178 (2003).
82. Lovett, M. *et al.* Silk fibroin microtubes for blood vessel engineering. *Biomaterials* **28,** 5271–5279 (2007).
83. Keten, S. & Buehler, M. J. Geometric confinement governs the rupture strength of H-bond assemblies at a critical length scale. *Nano Lett.* **8,** 743–748 (2008).
84. MacPhee, C. E. & Dobson, C. M. Formation of mixed fibrils demonstrates the generic nature and potential utility of amyloid nanostructures. *J. Am. Chem. Soc.* **122,** 12707–12713 (2000).
85. Reches, M. & Gazit, E. Casting metal nanowires within discrete self-assembled peptide nanotubes. *Science* **300,** 625–627 (2003).
Directing metal deposition through self-assembling peptide scaffolds.
86. Carny, O., Shalev, D. E. & Gazit, E. Fabrication of coaxial metal nanocables using a self-assembled peptide nanotube scaffold. *Nano Lett.* **6,** 1594–1597 (2006).
87. Lu, W. & Lieber, C. M. Nanoelectronics from the bottom up. *Nature Mater.* **6,** 841–850 (2007).
88. Scheibel, T. *et al.* Conducting nanowires built by controlled self-assembly of amyloid fibers and selective metal deposition. *Proc. Natl Acad. Sci. USA* **100,** 4527–4532 (2003).
Synthesis of metallic nanowires through self-assembling peptide scaffolds.
89. Niu, L. J., Chen, X. Y., Allen, S. & Tendler, S. J. B. Using the bending beam model to estimate the elasticity of diphenylalanine nanotubes. *Langmuir* **23,** 7443–7446 (2007).
90. Reches, M. & Gazit, E. Controlled patterning of aligned self-assembled peptide nanotubes. *Nature Nanotech.* **1,** 195–200 (2006).
91. Adler-Abramovich, L. *et al.* Self-assembled arrays of peptide nanotubes by vapour deposition. *Nature Nanotech.* **4,** 849–854 (2009).
92. Hamley, I. W. *et al.* Alignment of a model amyloid peptide fragment in bulk and at a solid surface. *J. Phys. Chem. B* **114,** 8244–8254 (2010).
93. Knowles, T. P. J., Oppenheim, T., Buell, A. K., Chirgadze, D. Y. & Welland, M. E. Nanostructured biofilms from hierarchical self-assembly of amyloidogenic proteins. *Nature Nanotech.* **5,** 204–207 (2010).
94. Barrau, S. *et al.* Integration of amyloid nanowires in organic solar cells. *Appl. Phys. Lett.* **93,** 023307 (2008).
95. Channon, K. J., Devlin, G. L. & MacPhee, C. E. Efficient energy transfer within self-assembling peptide fibers: A route to light-harvesting nanomaterials. *J. Am. Chem. Soc.* **131,** 12520–12521 (2009).
96. Liang, Y. *et al.* Light harvesting antenna on an amyloid scaffold. *Chem. Commun.* 6522–6524 (2008).
97. Maji, S. K. *et al.* Amyloid as a depot for the formulation of long-acting drugs. *PLoS Biol.* **6,** e17 (2008).
98. Holmes, T. C. *et al.* Extensive neurite outgrowth and active synapse formation on self-assembling peptide scaffolds. *Proc. Natl Acad. Sci. USA* **97,** 6728–6733 (2000).
99. Ellis-Behnke, R. G. *et al.* Nano neuro knitting: Peptide nanofiber scaffold for brain repair and axon regeneration with functional return of vision. *Proc. Natl Acad. Sci. USA* **103,** 5054–5059 (2006).
Refs 98 and 99: tissue engineering using amyloid scaffolds.
100. Gras, S. L. *et al.* Functionalised amyloid fibrils for roles in cell adhesion. *Biomaterials* **29,** 1553–1562 (2008).
101. Gimona, M. Protein linguistics - a grammar for modular protein assembly? *Nature Rev. Mol. Cell Biol.* **7,** 68–73 (2006).
102. Diaz-Avalos, R. *et al.* Cross-beta order and diversity in nanocrystals of an amyloid-forming peptide. *J. Mol. Biol.* **330,** 1165–1175 (2003).
103. Hemingway, E. *The Old Man and the Sea* (Vintage Books, 2007).
104. Nelson, R. *et al.* Structure of the cross-β spine of amyloid-like fibrils. *Nature* **435,** 773–778 (2005).
105. Galkin, V. E., Orlova, A., Cherepanova, O., Lebart, M-C. & Ebelman, E. H. High-resolution cryo-EM structure of the F-actin-fimbrin/plastin ABD2 complex. *Proc. Natl Acad. Sci. USA* **105,** 1494–1498 (2008).
106. Li, H., DeRosier, D. J., Nicholson, W. V., Nogales, E. & Downing, K. H. Microtubule structure at 8 A resolution. *Structure* **10,** 1317–1328 (2002).

Acknowledgements

T.P.J.K. acknowledges support from St John's College, Cambridge. M.J.B. acknowledges support from the Office of Naval Research (YIP and PECASE Awards), National Science Foundation (CAREER), Army Research Office and the Air Force Office of Scientific Research. We also acknowledge helpful discussions with D. Kaplan, A. Aguzzi, L. Luheshi, D. White and C. Dobson.

Additional information

The authors declare no competing financial interests.